Validation of the NG-18 Equations for Thick Walled Pipelines

C. J. Lyons[a,b,*], J. M. Race[c] , E. Chang[c], A. Cosham[d], B. Wetenhall[a], and J. Barnett[e]

[a] School of Engineering, Newcastle University, Armstrong Building, Queen Victoria Road, Newcastle upon Tyne, NE1 7RU, UK

[b] Pipeline Integrity Engineers Ltd., 262A Chillingham Road, Heaton, Newcastle upon Tyne, NE6 5LQ, UK

[c] Department of Naval Architecture, Ocean and Marine Engineering, University of Strathclyde, Henry Dyer Building, 100 Montrose Street, Glasgow, G4 0LZ, UK

[d] Ninth Planet Engineering Limited, Newcastle upon Tyne, NE6 1TT, UK

[e] National Grid, 35 Homer Road, Solihull, West Midlands, B91 3QJ, UK

ABSTRACT

The applicability of the flow stress dependent NG-18 equations to thick wall pipelines such as those used to transport dense phase carbon dioxide (CO_2) is demonstrated. A comparison between the components of the NG-18 equations and BS 7910 shows that the factor M_T for though-wall defects and M_P for part-wall defects in the NG-18 equations are very close to the reference stress solutions in BS 7910 Annex P, which are applicable to thick wall pipe. Thus, by inference, the flow stress dependent form of the NG-18 equations is also applicable to thick wall pipe. A further comparison with experimental failure data for thick wall pipes shows that the flow stress dependent NG-18 equations are applicable to wall thicknesses of up to 47.2 mm when the full-size equivalent upper shelf Charpy V-notch impact energy is at least 50 J. The results suggest that in principle, the flow stress dependent NG-18 equations may be used as limit state functions in models to calculate the failure frequency due to third party external interference, for high toughness, thick wall pipelines such as those required for dense phase CO_2 pipelines.

The Don Valley Power Project is co-financed by the European Union's European Energy Programme for Recovery
The sole responsibility of this publication lies with the author.
The European Union is not responsible for any use that may be made of the information contained therein.

Keywords

Fracture, Plastic collapse, Toughness, NG-18 equations, Thick wall pipe, CO_2 pipelines

1. INTRODUCTION

Carbon Capture and Storage (CCS) has been identified as an enabling technology to reduce carbon dioxide (CO_2) emissions into the atmosphere and meet international climate change

* Corresponding author: Tel: (0044)191 276 5300; E-mail: chris.lyons@pieuk.co.uk

commitments (Department for Business, Energy & Industrial Strategy, 2017). CCS involves the capture of CO_2 from large scale industrial emitters, and its transportation to geological sites for permanent storage. The most efficient method of transporting captured CO_2 is by pipeline in the dense phase (Downie, Race and Seevam, 2007). The aim of the research programme, COOLTRANS (CO2Liquid pipeline TRANSportation), led by National Grid, was to develop the knowledge base necessary to allow the safe design, construction and operation of an onshore dense phase CO_2 pipeline in the United Kingdom (UK) (Cooper and Barnett, 2014).

CO_2 is a hazardous substance which, in the unlikely event of an accidental release, could cause people harm. Therefore, an important consideration for the operation of an onshore CO_2 pipeline is to control the risk that the pipeline presents to the public. Quantitative risk assessment (QRA) involves the analysis of the frequency and consequences of a pipeline failure. It provides an assessment of the individual and societal risk to the nearby populations, and determines whether mitigating action is required to reduce the risk (IGEM, 2013). The method required for the QRA of dense phase CO_2 pipelines was developed as part of the COOLTRANS research programme.

Calculation of the frequency of pipeline failure from each credible failure mechanism is a fundamental part of pipeline QRA. Historically, mechanical damage through third party external interference is the largest individual cause of pipeline failure in the UK and therefore represents the greatest risk to the surrounding population (UKOPA, 2019). Buried transportation pipelines are installed in third party land, and therefore may be subject to interference damage as a result of activities carried out by third parties in the vicinity of the pipeline. The frequency of pipeline failure due to third party mechanical damage is calculated using probabilistic structural reliability methods, combining operational data on pipeline damage with semi-empirical fracture mechanics failure equations. This approach has been employed for over 25 years, is tried and tested, and is well understood (Corder et al., 1992)(Corder, 1995).

To calculate the pipeline failure frequency due to third party external interference for dense phase CO_2 pipelines, it would be desirable to extend the use of the established failure frequency method.

Existing third-party external interference failure frequency models, for oil and gas pipelines, were reviewed in a recent study (Lyons et al., 2019) in order to assess whether they could be applied to dense phase CO_2 pipelines. The review covered FFREQ (Corder et al., 1992), PIPIN (HSE, 2001), PIE (Lyons, 2008) and Cosham (Cosham, 2008) models, and an update to the pipeline damage probability distributions (Goodfellow, Turner, Haswell and Espiner, 2012).

It was noted by the review (Lyons et al., 2019), that operational pipeline damage data used within the existing failure frequency models is restricted to existing UK pipelines with standard wall thicknesses, i.e. up to 19.1 mm for the line pipe used at road/rail crossings.

Furthermore, the fracture mechanics failure equations used in the failure frequency models, namely the NG-18 equations, used to calculate gouge failure and leak/rupture; and the British Gas Dent Gouge Model, used to calculate gouged dent failure, are semi-empirical. The experimental test data used in the derivation of these equations also predominantly concerns standard pipeline wall thicknesses with upper limits of 21.9 mm and 15.6 mm for through-wall and part-wall gouge defects respectively, and 16.4 mm for gouged dent defects (Lyons et al., 2019).

Dense phase CO_2 pipelines have a high design pressure requirement (Noothout et al., 2014), this typically necessitates the use of line pipe with a wall thickness greater than the values indicated above. It was therefore concluded by the review (Lyons et al., 2019) that the wall thickness of typical dense phase CO_2 pipelines would be beyond the known range of applicability of the operational data and failure equations used for the established failure frequency method.

This paper presents a detailed validation study to assess whether the fracture mechanics failure equations used to calculate gouge failure for the established failure frequency method, the NG-18 equations, may also be applied to thick wall pipelines such as those used for dense phase CO_2 transportation. Note that throughout this paper the term "thick wall" is used to denote a wall thickness in excess the upper limits used in the experimental tests performed as part of the formulation of the NG-18 equations, specifically 21.9 mm for through-wall defects and 15.6 mm for part-wall defects. The study consists of two parts, firstly, a comparison is made between the component parts of the NG-18 equations and the BS 7910 defect assessment method, which is applicable to thick wall pipe, in order to show the similarities and differences between them in terms of their basic structure. The component parts are illustrated graphically in order to show the effect of increased wall thickness. Secondly, a comparison between experimental failure data for thick wall cylindrical pressure vessels and failure predictions calculated using the NG-18 equations is made to show the accuracy of the equations. The NG-18 equations and the relevant sections of BS 7910 are described in Section 2, the comparison between NG-18 and BS 7910 is presented in Section 3 and the comparison between prediction and experimental data is presented in Section 4.

2. THE NG-18 EQUATIONS AND BS 7910 ASSESSMENT METHOD

External interference failure frequency models use limit state functions to define the conditions for pipeline failure in terms of defect size, pipeline geometry, and the material properties of the line pipe steel. Existing failure frequency models, using the established failure frequency method, employ the through-wall and part-wall NG-18 equations (Kiefner, Maxey, Eiber and Duffy, 1973) as the limit state functions (Lyons et al, 2019) for leak/rupture and gouge failure respectively.

The NG-18 equations are semi-empirical and pipeline specific. They were derived and calibrated using the experimental results of burst and material tests on pipe specimens over

a range of geometries and properties which would be expected for normal pipeline operation at the time, i.e. on through-wall defects in pipe up to 21.6 mm thick and on part-wall defects in pipe up to 15.6 mm (Lyons et al., 2019). Validation of the use of the NG-18 equations for thick wall pipelines forms the basis of this study.

The British Standard BS 7910 (BSI, 2013) includes a more general assessment method for defects in metallic structures, which can be applied to both thin wall and thick wall pipe. This section describes the NG-18 equations and the parts of BS 7910 relevant to a comparison between the two.

2.1 THE NG-18 EQUATIONS

The NG-18 equations were developed through the 1960s and early 70s by the Battelle Memorial Institute (Hahn, Sarrate and Rosenfield, 1969) (Kiefner, 1969) (Maxey, Kiefner, Eiber and Duffy, 1972) (Kiefner, Maxey, Eiber and Duffy, 1973) to describe a longitudinally orientated defect in a cylinder subject to internal pressure loading. Based upon the operating conditions of a pipeline, the through-wall NG-18 equations are used to determine whether an axially oriented through-wall defect will lead to a full-bore rupture or remain as a leak, while the part-wall NG-18 equations are used to determine whether an axially oriented part-wall defect (i.e. a gouge) will progress into a through-wall defect.

Both the through-wall and part-wall NG-18 equations exist in two forms: toughness dependent and flow stress dependent. They are listed as follows for through-wall defects:

Toughness dependent form

$$\frac{K_C^2 \pi}{8c\overline{\sigma}^2} = \ln \sec\left(\frac{\pi M_T \sigma_H}{2\overline{\sigma}}\right) \tag{1}$$

Flow stress dependent form

$$\sigma_H = {M_T}^{-1}\overline{\sigma} \tag{2}$$

where K_C is the material's fracture toughness, c is half of the axial defect length, σ_H is the circumferential hoop stress at failure, $\overline{\sigma}$ is the flow stress (which is a measure of the stress at which unconstrained plastic flow occurs) and, M_T is the Folias factor, which accounts for the bulging which occurs when a defect is present in a pressurised pipeline.

The toughness dependent and flow stress dependent forms of the part-wall NG-18 equation use a correction to the Folias factor, M_P, in place of M_T:

$$M_P = \left[\frac{1 - \frac{d}{t}\left(\frac{1}{M_T}\right)}{1 - \frac{d}{t}}\right] \quad (3)$$

where d is the depth of the part-wall defect and t is the pipe wall thickness.

For the purpose of this study, the Folias factor (Folias, 1975) used in the NG-18 equations is the 2-term expression applicable to long defects:

$$M_T = \sqrt{1 + 0.26\left(\frac{2c}{\sqrt{Rt}}\right)^2} \quad (4)$$

where R is the external radius of the pipeline.

The empirical flow stress (Corder et al., 1992)(Corder, 1995) used is given by:

$$\bar{\sigma} = 1.15\sigma_Y \quad (5)$$

where σ_Y is the yield strength of the structure. Although they are not the original terms used for the NG-18 equations, the use of the above expressions in this study results from their historical use in the established failure frequency method (Lyons, 2008).

For the toughness dependent NG-18 equations, the material fracture toughness value K_c is determined using a correlation with the Charpy V-notch energy. This correlation was empirically derived using experimental data and is as follows:

$$K_C^2 = C_v \frac{E}{A} \quad (6)$$

where C_v is the 2/3 Charpy V-notch upper shelf impact energy, A is the fracture area of the Charpy specimen, and E is the Young's Modulus of steel.

2.2 BS 7910

BS 7910 defect assessments are performed using a Failure Assessment Diagram (FAD) approach. This method is derived from fracture mechanics theory and considers that failure of the structure can occur due to either fracture or plastic collapse. Based on the geometry of the structure, its operating conditions and the dimensions of the defect, two separate quantities are calculated, one representing fracture and one representing plastic collapse.

The quantity representing fracture is known as the fracture ratio, K_r:

$$K_r = \frac{K_I}{K_{mat}} \tag{7}$$

where K_{mat} is the material fracture toughness and K_I is the stress intensity factor. The form of the stress intensity factor is dependent on the type and the dimensions of the defect and the geometry and operating conditions of the structure being assessed.

The general form of the stress intensity factor is:

$$K_I = (Y\sigma)\sqrt{\pi a} \tag{8}$$

where, a, is half the defect length in the case of a through-wall defect, or the defect depth in the case of a part-wall defect; Y is a function which depends on the geometry; and σ is the applied stress.

The stress is linearised into membrane and bending components, i.e. P_m and P_b, using the expressions in Figure 2 of BS 7910 (BSI, 2013).

Yσ in Equation (8) is given by equations (M.3), (M.4) (M.5) in Annex M of BS 7910 (BSI, 2013). Note that for the purposes of the comparison, secondary stresses are assumed to be zero. The factors due to regions of local stress concentration, structural discontinuities and misalignment (M_{km}, M_{kb}, k_t, k_{tm}, k_{tb}, k_m) are taken to be equal to 1. The finite width correction factor, f_w, is calculated using the expressions given in Section M.2 of BS 7910. The typical length of a section of line pipe of 12 m is assumed in this study.

For the case of a through-wall defect, Equation (M.21) from Section M.6.1 of BS 7910 (BSI, 2013) for curved shells under internal pressure, is used to calculate the bulging correction factor. The membrane and bending load factors, M_m and M_b respectively, are taken from Section M.3.1 of BS 7910.

For the case of a part-wall defect, Equation (M.22) from Section M.6.1 of BS 7910 (BSI, 2013) is used to calculate the bulging correction factor and the membrane and bending load factors from Section M.6.2 of BS 7910 (BSI, 2013) are used. These include the flat-plate solutions from BS 7910 Section M.4.1.2 for the membrane term M_m and BS 7910 Section M.4.1.3 for the bending term M_b.

It should be noted that different expressions for the flow stress and Folias factor are used in the BS 7910 assessment method. Note also, that BS 7910 uses the term “flow strength” in place of “flow stress”.

The flow strength in BS 7910 is defined as the average of the yield strength and the tensile strength:

$$\bar{\sigma} = \frac{\sigma_Y + \sigma_U}{2} \tag{9}$$

where σ_U is the tensile strength of the structure.

The Folias factor is defined in BS 7910 using the following two-term expression:

$$M_T = \sqrt{1 + 0.40\left(\frac{2c}{\sqrt{Rt}}\right)^2} \tag{10}$$

For comparison purpose, the external radius of the pipeline is used to calculate the Folias factor for stress intensity factors and reference stresses using BS 7910 method.

In BS 7910, the quantity representing plastic collapse is known as the load ratio, L_r:

$$L_r = \frac{\sigma_{ref}}{\sigma_Y} \tag{11}$$

where σ_{ref} is the reference stress which is dependent on the type and dimensions of the defect and the geometry and operating conditions of the structure being assessed.

For the reference stress term in the load ratio, Equation (P.17) from Section P.9.1 in Annex P of BS 7910 is used for the through-wall defect case and Equation (P.18) from BS 7910 Section P.9.2 is used in accordance with Section P.9.4 for the external part-wall defect case. In Equations (P.17) and (P.18), the factor of 1.2 which occurs in the first term of both equations has not been applied. This factor was originally introduced in order to increase the level of conservatism in the reference stress solutions for curved shells and therefore a more accurate comparison with the NG-18 equations can be achieved by ignoring it.

Once the specific fracture ratio (K_r) and load ratio (L_r) for the defect and structure have been calculated, they can be plotted as a point on a FAD. If the calculated values of K_r and L_r lie within the failure assessment line, then the defect is considered acceptable.

3 FAILURE MODEL COMPARISON

3.1 COMPONENT ANALYSIS

The defect assessment code PD 6493:1991 (BSI, 1991) was a precursor to BS 7910. If the equation for the FAD in PD 6493 Level 2 is considered:

$$K_r = S_r\left\{\frac{8}{\pi^2}\ln\sec\left(\frac{\pi}{2}S_r\right)\right\}^{-0.5} \tag{12}$$

It can be seen that this is very similar to the toughness dependent NG-18 equations (Equation (1)). This is because the NG-18 equations and the Level 2 FAD in PD 6493:1991 (BSI, 1991) are both based on the Dugdale strip yield model. Note that in Equation (12), the load ratio S_r is similar to L_r but instead uses the flow stress in place of the yield strength.

The toughness dependent NG-18 equations may therefore be expressed in the form of a FAD with equivalent fracture and plastic collapse terms. If we consider the toughness dependent form of the through-wall NG-18 equation (Equation (1)), this can be rearranged as follows (Cosham, Hopkins and Leis, 2012):

$$K_c^2 = c\overline{\sigma}^2 \frac{8}{\pi} \ln\left[\sec\left(\frac{\pi}{2}\left\{\frac{M_T\sigma_H}{\overline{\sigma}}\right\}\right)\right] \tag{13a}$$

$$\left\{\frac{M_T\sigma_H\sqrt{\pi c}}{K_c}\right\} = \left\{\frac{M_T\sigma_H}{\overline{\sigma}}\right\}\left\{\frac{8}{\pi^2}\ln\left[\sec\left(\frac{\pi}{2}\left\{\frac{M_T\sigma_H}{\overline{\sigma}}\right\}\right)\right]\right\}^{-\frac{1}{2}} \tag{13b}$$

If the left hand side of Equation (13b) is defined as the fracture ratio, K_r, and the expression $\left\{\frac{M_T\sigma_H}{\overline{\sigma}}\right\}$ on the right hand side is defined as the load ratio, S_r, then the equation becomes:

$$K_r = S_r\left\{\frac{8}{\pi^2}\ln\sec\left(\frac{\pi}{2}S_r\right)\right\}^{-\frac{1}{2}} \tag{13c}$$

The failure assessment line implied within the toughness dependent NG-18 equations is therefore identical to that of PD 6493 (Equation (12)).

A comparison of the stress intensity factor and reference stress solutions in BS 7910 with the equivalent terms in Equation (13b) is shown in Table 1.

BS 7910	**NG-18**
Stress Intensity Factor	
$K_I = (Y\sigma)\sqrt{\pi a}$ ((Yσ) from Equations (M.3), (M.4), (M.5), (M.21) and Sections M.6.1 and M.3.1 from Annex M of BS 7910)	$K_I = (M_T\sigma_H)\sqrt{\pi c}$ (Implied by Equation (13b))
Reference Stress	
$\sigma_{ref} = M_T P_m + \frac{2P_b}{3\left(1-\frac{2a}{W}\right)}$ (Equation P.17 in Section P.9.1 from Annex P of BS 7910)	$\sigma_{ref} = M_T\sigma_H$ (implied by Equation (13b) and $S_r - L_r$ relationship)

Table 1: Fracture and Plastic Collapse Components from BS 7910 and the Toughness Dependent Through-Wall NG-18 Equation

In Table 1, W is the structure width in the defect plane. It can be seen from this table that firstly, the Folias factor, M_T, in the NG-18 equation is equivalent to the function Y in BS 7910. Secondly, the product of the Folias factor and hoop stress in the NG-18 equation, $M_T\sigma_H$, is equivalent to the reference stress, σ_{ref}, in BS 7910.

For through-wall defects, both methods have similar expressions for the stress intensity factor, K_I, and the reference stress, σ_{ref}. However, different formulae are used to calculate the Folias factor M_T, as described in Sections 2.1 and 2.2. For the stress intensity factor, the difference

between section M.6.1 in BS 7910 and the NG-18 equation is the finite width correlation factor, f_w. For the reference stress, the difference between Equation P.17 in BS 7910 and the NG-18 equation is the inclusion of the bending stress, P_b.

A similar analysis can be performed using the part-wall NG-18 equation. The respective stress intensity and reference stress components from BS 7910 and NG-18 for part-wall defects are shown in Table 2.

BS 7910	**NG-18**
Stress Intensity Factor	
$K_I = (Y\sigma)\sqrt{\pi a}$ ((Yσ) from Equations (M.3), (M.4), (M.5), (M.22), Sections M.4.1.2 and M.4.1.3 from Annex M of BS 7910)	$K_I = (M_P\sigma_H)\sqrt{\pi d}$ (implied by Equation (1) and analysis from Equations (13a) to (13b))
Reference Stress	
$\sigma_{ref} = M_S P_m + \frac{2P_b}{3(1-\alpha'')^2}$ (Equation P.18 from Annex P of BS 7910)	$\sigma_{ref} = M_P\sigma_H$ (implied by Equation (1), analysis from Equations (13a) to (13b) and $S_r - L_r$ relationship)

Table 2: Fracture and Plastic Collapse Components from BS 7910 and the Toughness Dependent Part-Wall NG-18 Equation

In Table 2, the parameter α'' is defined in Appendix P9 of BS 7910 (BSI, 2013). The comparison for part-wall defects shows that the stress intensity factors are significantly different for the two methods. M_p in the NG-18 equation is an empirical term. Its derivation indicates that it is not appropriate to use to calculate the stress intensity factor. However, for the reference stress, M_s in BS 7910 is very similar to M_p in the NG-18 equation. The difference between Equation P.18 and the NG-18 equation is the inclusion of the bending stress, P_b.

While the structure of the toughness dependent form of the through-wall NG-18 equation is similar to that of BS 7910, the toughness dependent part-wall equation is not recommended for the calculation of part-wall defect failure because the stress intensity factor is not appropriate.

Comparison of the reference stresses show that M_T and M_P in the NG-18 equations are very similar to the equivalent terms in the reference stress solutions in BS 7910 Annex P, which are applicable to thick wall pipe. The main difference between them is that BS 7910 includes both the membrane stress, P_m, and the bending stress, P_b, whilst the NG-18 equations only include the membrane stress. By inference, M_T and M_P are therefore applicable to thick wall pipe and, provided the effect of the bending stress remain small, the flow stress dependent form of the NG-18 equations are also applicable to thick wall pipe. The effect of the bending stress is considered in Section 3.2.

It should be noted that the correlations between the material fracture toughness and the Charpy V-notch impact energy in BS 7910 differ significantly from the correlation used in the NG-18 equations. The correlations in BS 7910 are very conservative because they are intended to be used when no measured fracture toughness data are available and are intended to give a lower bound estimate of the fracture toughness. They also cover materials other than line pipe. By contrast, the correlation in the NG-18 equations is empirical. The fracture toughness was calculated using the results of tests on through-wall defects rather than using high-constraint fracture mechanics test specimens. Therefore, the correlation might not be applicable to thick wall pipe. As toughness increases, the burst strength tends to a toughness independent, or flow stress dependent, form representing the plastic collapse limit state. If defect failure in the line pipe used in pipeline construction is controlled by plastic collapse rather than fracture, then the flow stress dependent form of the NG-18 equations would be the most appropriate for application to high toughness steel.

For the flow stress dependent NG-18 equations to be applicable, the steel must have a high enough toughness such that the failure is controlled by plastic collapse. According to both IGEM/TD/1 Edition 5 (2016) and PD 8010 (BSI, 2015), drop weight tear testing (DWTT) requirements should be applied to pipe with a diameter greater than or equal to 323.9 mm in order to assess resistance to prevent propagating brittle fracture. The fracture propagation transition temperature is defined by the 85% shear appearance transition temperature (SATT) from the DWTT. The fracture propagation transition temperature is higher than the fracture initiation transition temperature. The DWTT specimen is a full-thickness test specimen. The requirement for the DWTT testing ensures that line pipe is on the upper shelf. The failure of a part or through-wall defect will be ductile. That is not, however, necessarily sufficient for failure to be controlled by plastic collapse. That depends on the upper shelf Charpy V-notch impact energy. The toughness necessary for failure to be controlled by plastic collapse remains undefined, which will be subject to further study.

It is therefore concluded that in principle, the flow stress dependent NG-18 equations would be suitable for application to thick wall CO_2 pipelines, provided the pipe material was of a high toughness.

3.2 GRAPHICAL ILLUSTRATION WITH WALL THICKNESS

In order to illustrate the similarities and differences between the BS 7910 and NG-18 approaches, comparisons have been made between the stress intensity factor, K_I and reference stress, σ_{ref} for each assessment method, considering both through-wall and part-wall defects. The comparisons show the variation in each component with increasing wall thickness for a range of defect dimensions.

The pipeline parameters used in the comparison, are shown in Table 3. Two different external diameters, i.e. 610mm and 914mm, with the same material properties and design factor are considered. The pressure was calculated using Lamé's equation for the hoop stress in a thick

289 wall cylinder (Lamé and Clapeyron, 1833) such that the stress at the internal pipe wall always
290 remains at a value of 72 percent of the specified minimum yield strength.

Input	Value
External Diameter (mm)	610, 914
Material Grade	L450
Specified Minimum Yield Strength (Nmm^{-2})	450
Specified Minimum Tensile Strength (Nmm^{-2})	535
full-size equivalent Charpy V-Notch Impact Energy (J)	100
Design Factor	0.72

291 **Table 3:** Pipeline Parameters for NG-18 and BS 7910 Comparison

292 To select a range of defect dimensions to be used in each comparison case, the United
293 Kingdom Onshore Pipeline Operators' Association (UKOPA) Pipeline Fault Database (UKOPA,
294 2019) was consulted. This database contains records of third party damage incidents affecting
295 gas and liquid pipelines in the UK and gives information on specific defect dimensions. The
296 dimensions of three through-wall defects and three part-wall defects were chosen directly
297 from the database. Three variations are included, a shallow long defect, a mid length and mid
298 depth defect and a short deep defect. Note that the depths of the part-wall defects are
299 represented in the comparisons as a percentage of wall thickness. As wall thickness increases,
300 defect dimensions may not be representative of realistic defects which could occur as a result
301 of third-party external interference. The purpose of the comparisons is to observe the effect
302 of the differences between NG-18 and BS 7910 with increasing wall thickness. The dimensions
303 of the through-wall and part-wall defects are shown in Table 4 and Table 5:

Defect No.	Length (mm)
1	203
2	89
3	5

304 **Table 4:** Through-Wall Defect Dimensions for NG-18 and BS 7910 Comparison

Defect No.	Length (mm)	Depth (% wall thickness)
1	1350	14
2	480	54
3	20	63

305 **Table 5:** Part-Wall Defect Dimensions for NG-18 and BS 7910 Comparison

Through-Wall Defects

For through-wall defects, the comparison has been performed using the three defects listed in Table 4 with pipeline parameters from Table 3. The results of the investigation are shown in Figure 1 and Figure 2. They are presented as the ratio of the value calculated using the NG-18 equations to the value calculated using BS 7910.

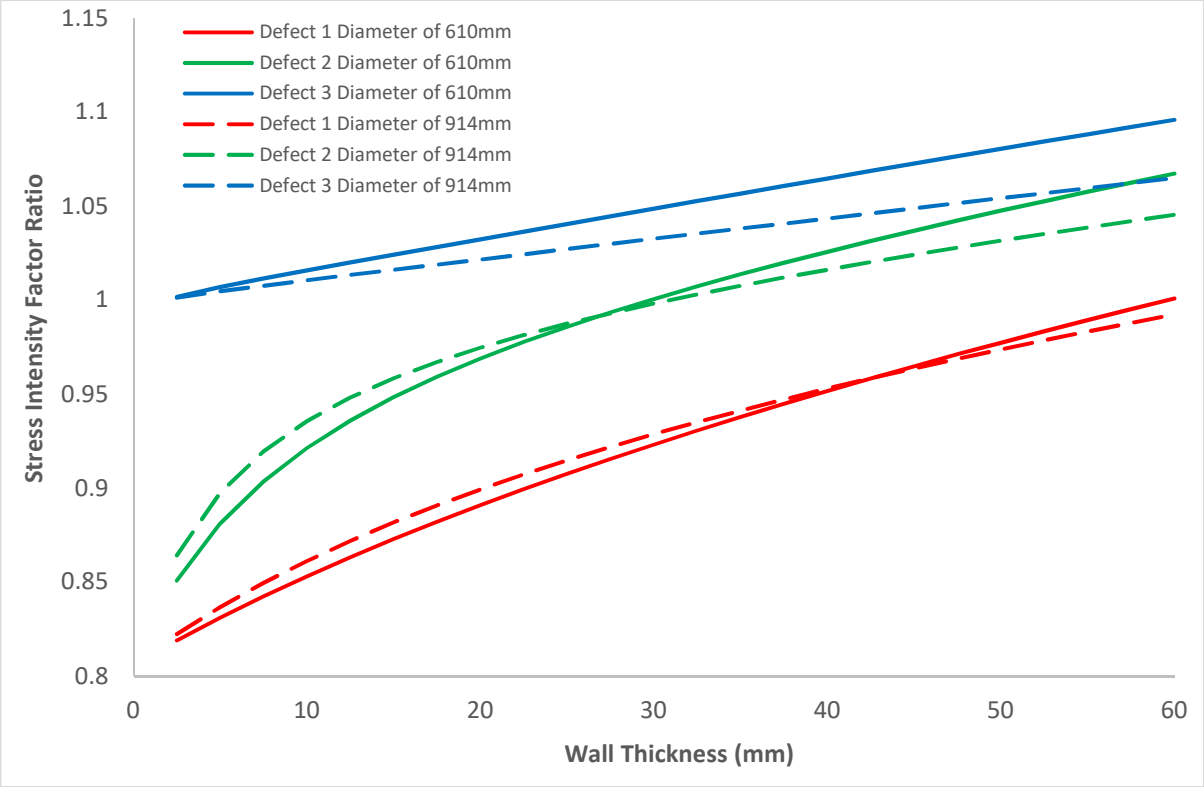

Figure 1 Stress Intensity Factor Ratio of NG-18 and BS 7910 with Increasing Wall Thickness for Three Different Axial Through-Wall Defects

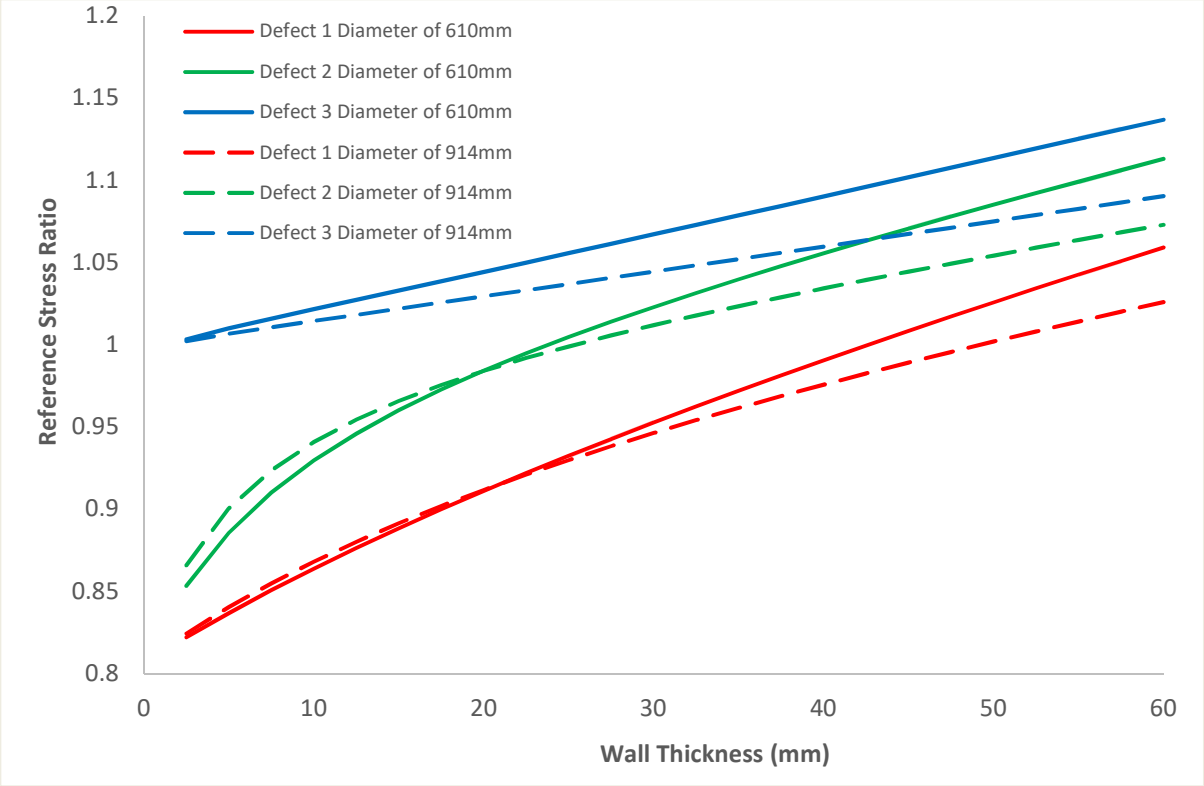

Figure 2 Reference Stress Ratio of NG-18 and BS 7910 with Increasing Wall Thickness for Three Different Axial Through-Wall Defects

The proximity of the data to unity in Figure 1 and Figure 2 illustrates the similarity between the stress intensity factors and reference stresses used in the through-wall NG-18 equations and BS 7910. Almost the same values are produced for each of the three defects investigated at all wall thicknesses considered with the differences remaining small. In the case of the stress intensity factor, the differences between the methods result from the presence of the bending stress and the finite width correction factor, f_w, in BS 7910; and the slightly different Folias factors used in each method.

In the case of the reference stress, the difference between the methods result from the presence of the bending stress in BS 7910 and the slightly different Folias factors used in each method. In each case at low wall thickness, the bending stress is very small. The difference between the methods therefore primarily results from the finite width correction factor (for stress intensity only) and the different Folias factors. The effect of the Folias factor is observed by the difference between the short, mid and long defects at low wall thickness. As wall thickness is increased, the bending stress increases, the increasing influence of these quantities with increasing wall thickness causes the trends shown in each ratio. Figure 1 and Figure 2 also show the effect of pipe diameter to be minor for the thickness range considered.

Part-Wall Defects

Similarly, a comparison was also made for part-wall defects using the three defects listed in Table 5 with pipeline parameters from Table 3. The results are shown in Figures 3 and 4.

For stress intensity factor, Defect 3, which is short and deep, shows large variation in the difference between the two methods with increasing wall thickness. At the lowest wall thickness considered the NG-18 stress intensity factor is approximately half that of the equivalent BS 7910 value. As wall thickness is increased, the relative size of the NG-18 value to BS 7910 also increases, such that at a wall thickness of 60 mm, it is between 4 and 5 times as large as the BS 7910 value for the diameters considered. For Defect 2, which is mid length, mid depth, the NG-18 stress intensity factor is lower than the BS 7910 equivalent for all wall thicknesses considered. Its value varies from approximately 0.3 times the BS 7910 equivalent at the lowest wall thickness to approximately 0.6 times the BS 7910 equivalent at 60 mm. Defect 1, which is long and shallow, shows the closest agreement between the two methods at all wall thicknesses considered. The comparison highlights that the stress intensity factor implied by the toughness dependent part-wall NG-18 equation is not appropriate.

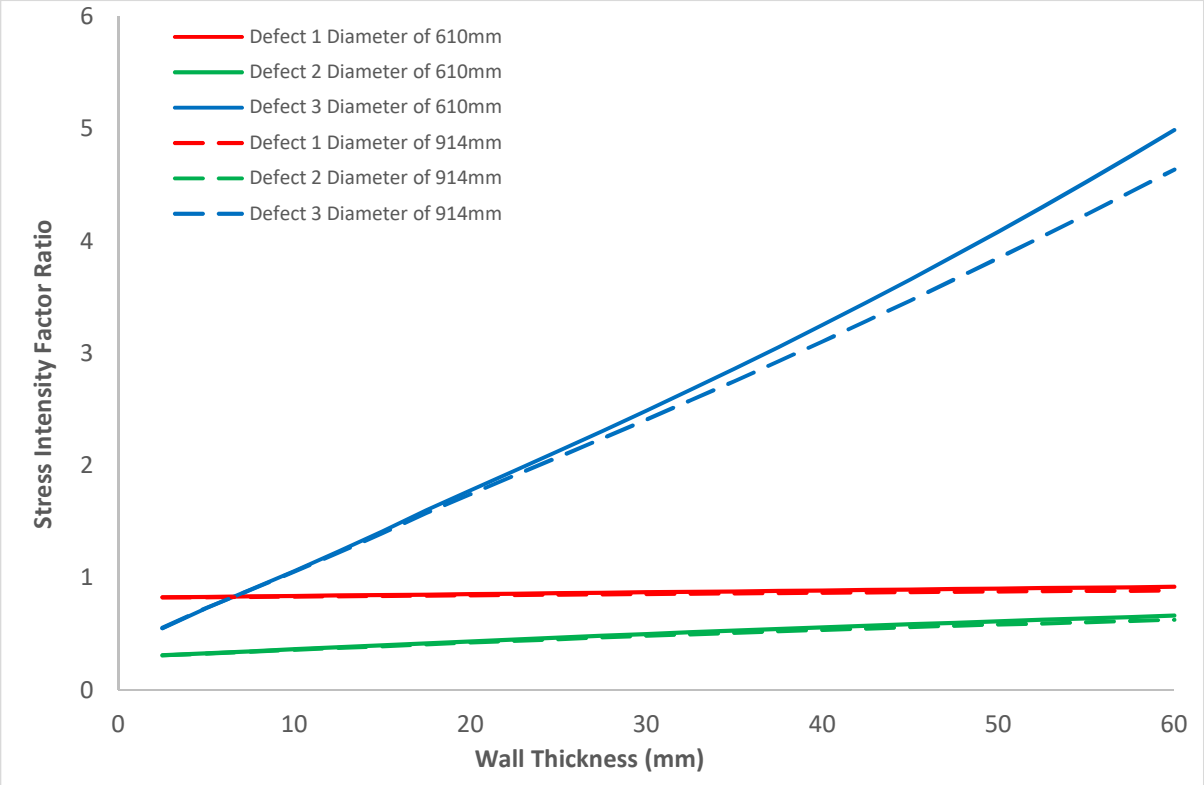

Figure 3 Stress Intensity Factor Ratio of NG-18 and BS 7910 with Increasing Wall Thickness for Three Different Axial Part-Wall Defects

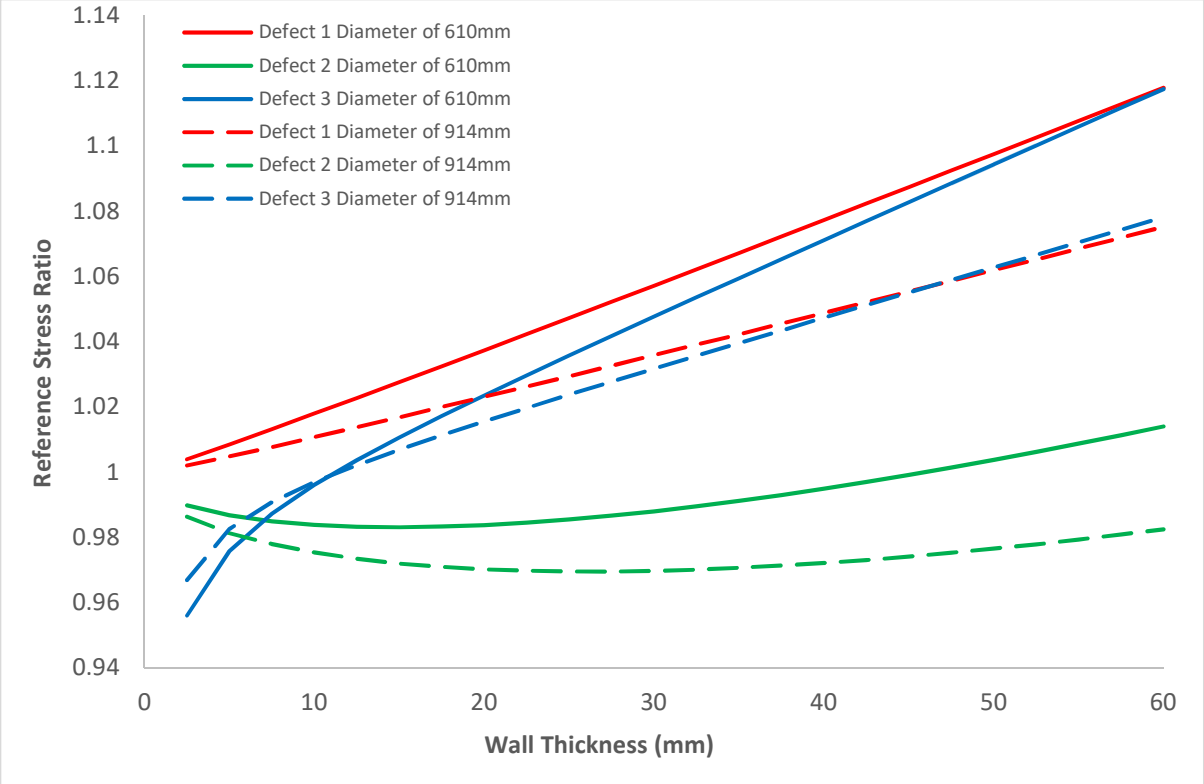

Figure 4 Reference Stress Ratio of NG-18 and BS 7910 with Increasing Wall Thickness for Three Different Axial Part-Wall Defects

For reference stress, similar to Figure 1 and Figure 2, the data is very close to unity for each of the wall thicknesses considered. This highlights the similarity between the reference stress solutions for each assessment method at all wall thicknesses considered, with the differences remaining small. The difference between the methods again result from the presence of the bending stress in BS 7910 and the slightly different Folias factors used in each method. At low wall thickness, the bending stress is small. The difference between the methods therefore primarily results from the different Folias factors. The effect of the Folias factor is observed by the difference between the short, mid and long defects at low wall thickness. As wall thickness is increased, the bending stress increases, the increasing influence of these quantities with increasing wall thickness causes the trends shown in each ratio. The effect of pipe diameter is shown to be minor for the thickness range considered.

In summary, the comparisons show that the reference stresses derived from the NG-18 equations are similar to those from BS 7910 for both through-wall and part-wall defects. The effect of the bending stress is small and remains small even when the pipeline wall thickness is increased. A similar effect is observed for the stress intensity factor for through-wall defects. However, the stress intensity factor implied by the toughness dependent part-wall NG-18 equation is not appropriate. In line with Section 3.1, it is concluded that the flow stress dependent form of the NG-18 equations are applicable to thick wall pipe.

4. COMPARISON WITH REAL FAILURE DATA

The above component analysis shows that the flow stress dependent form of the NG-18 equations would, in principle, be a suitable method to apply to thick wall CO_2 pipelines, provided that the pipe material was of a high toughness. However, in order to satisfactorily determine the accuracy of the flow stress dependent NG-18 equations when applied to thick wall pipelines, a comparison between predicted values of failure pressure and experimental test data is required. In this section, the predictions of both toughness and flow stress dependent forms of the NG-18 equations are compared with through-wall and part-wall defect burst tests on thick wall pipe sections and pressure vessels taken from a search of the available literature.

As explained in Section 3.1, the correlations between the fracture toughness and Charpy V-notch impact energy in BS 7910 are very conservative when compared to the correlation in the NG-18 equations. Consequently, predictions using BS 7910 are not included in this section. Comparisons with BS 7910 would only be informative if the fracture toughness was available.

4.1. THROUGH-WALL DEFECTS

4.1.1 THROUGH-WALL FAILURE DATA

The experimental failure data available for burst tests of through-wall defects on thick wall vessels originates from Sturm and Stoppler in 1990 (Sturm and Stoppler, 1990) (Staat, 2004). Three tests were performed on vessels constructed from 20 MnMoNi 55 grade manganese-molybdenum-nickel alloy steel (150 J) and one test was performed on a vessel constructed from 22 NiMoCr 37 mod nickel-molybdenum-chromium alloy steel (50 J). Details of the vessels and tests are summarised in Table 6.

Input	Value
External Diameter (mm)	798
Wall Thickness (mm)	47.2
Material Grade	20 MnMoNi 55, 22 NiMoCr 37 mod
Yield Strength (Nmm^{-2})	428, 417
Tensile Strength (Nmm^{-2})	605, 622
Charpy V-Notch Impact Energy (J) Full-Size	150, 50
Defect Length Range (2c) (mm)	650 – 1105

Table 6: Thick Wall, Through-Wall Burst Test Vessel Details, Sturm and Stoppler, 1990

Data from burst tests of through-wall defects on thin wall vessels have also been included in order to provide a comparison. This data originates from Battelle in 1973 (Kiefner, Maxey, Eiber and Duffy, 1973) and includes data from 90 burst tests of through-wall defects on thin wall pressure vessels. These tests were performed for a range of different vessels and parameters. Details are summarised in Table 7.

Input	Value
External Diameter Range (mm)	168 – 1219
Wall Thickness Range (mm)	4.9 – 21.9
Yield Strength Range (Nmm^{-2})	220 – 735
Tensile Strength Range (Nmm^{-2})	338 – 908
Charpy V-Notch Impact Energy (J) Full-Size	20 – 136
Defect Length Range (2c) (mm)	25 – 508

Table 7: Thin Wall, Through-Wall Burst Test Vessel Details, Kiefner et al., 1973

4.1.2. FAILURE DATA COMPARISON

Figure 5 shows predicted and actual failure stresses as a ratio of yield strength for the set of axial through-wall defects in thick wall pressure vessels (Table 6). The predictions are made using both the toughness and flow stress dependent forms of the NG-18 equations. Data points which lie below the line of unity are conservative, with the model predicting a failure stress below that of the experimental failure stress. The closer data points are to the line of unity, the more accurate the prediction of failure stress. The failure stress is assumed to be the hoop stress at the failure pressure.

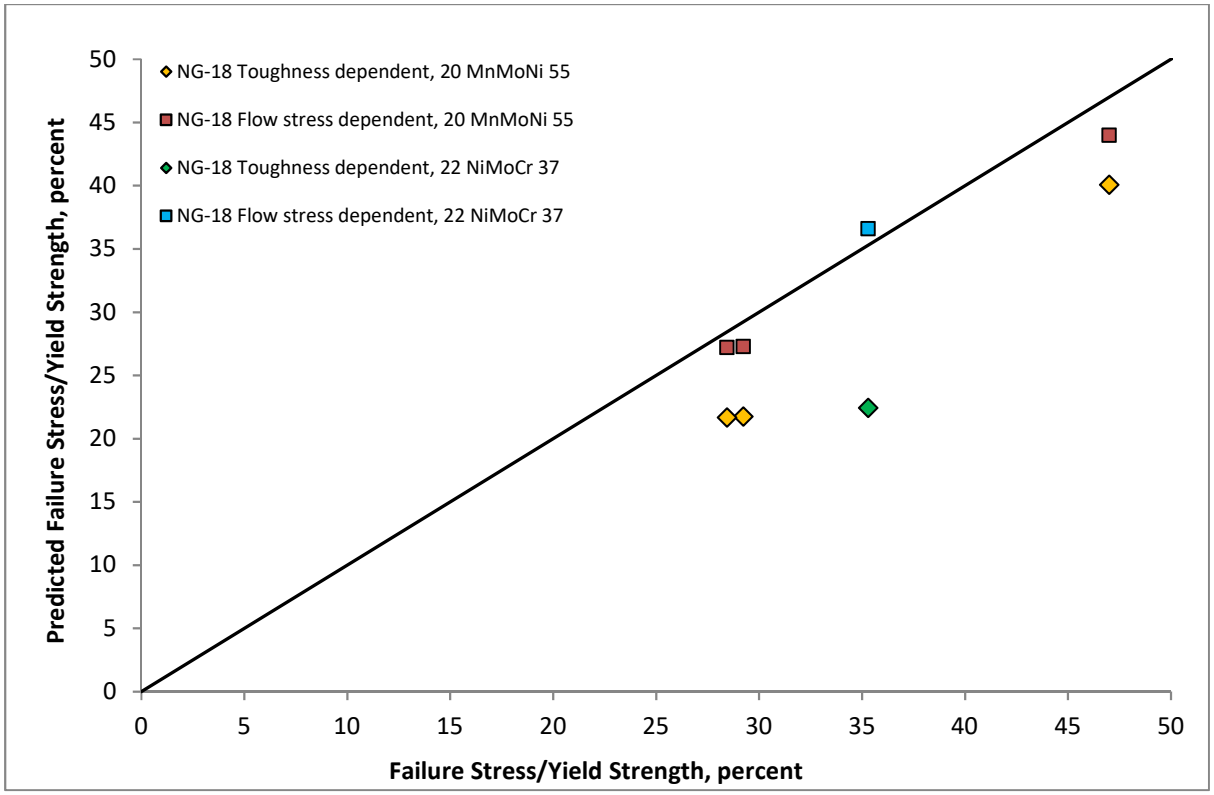

Figure 5 Predicted versus Actual Failure Stress for Axial Through-Wall Defects in Thick Wall Pipe Sections According to the Toughness and Flow Stress Dependent Forms of the NG-18 Equations, Sturm and Stoppler

Figure 5 shows that, for the tests considered, the predictions of the toughness dependent form of the NG-18 equation are more conservative than those of the flow stress dependent form. The failure stresses calculated by the flow stress dependent form of the NG-18 equation are between approximately 10% and 75% greater than those calculated by the toughness dependent form. Figure 5 shows the flow stress dependent NG-18 equation to be the more accurate method for calculating predictions of pipeline failure stress for through-wall defects in thick wall pipelines.

Figure 6 shows the same data from Figure 5 and also includes the results of burst tests on axial through-wall defects in thin wall pressure vessels from Battelle in 1973 (Table 7). This figure shows the thick wall data to be contained within the scatter of the data points of the thin wall data.

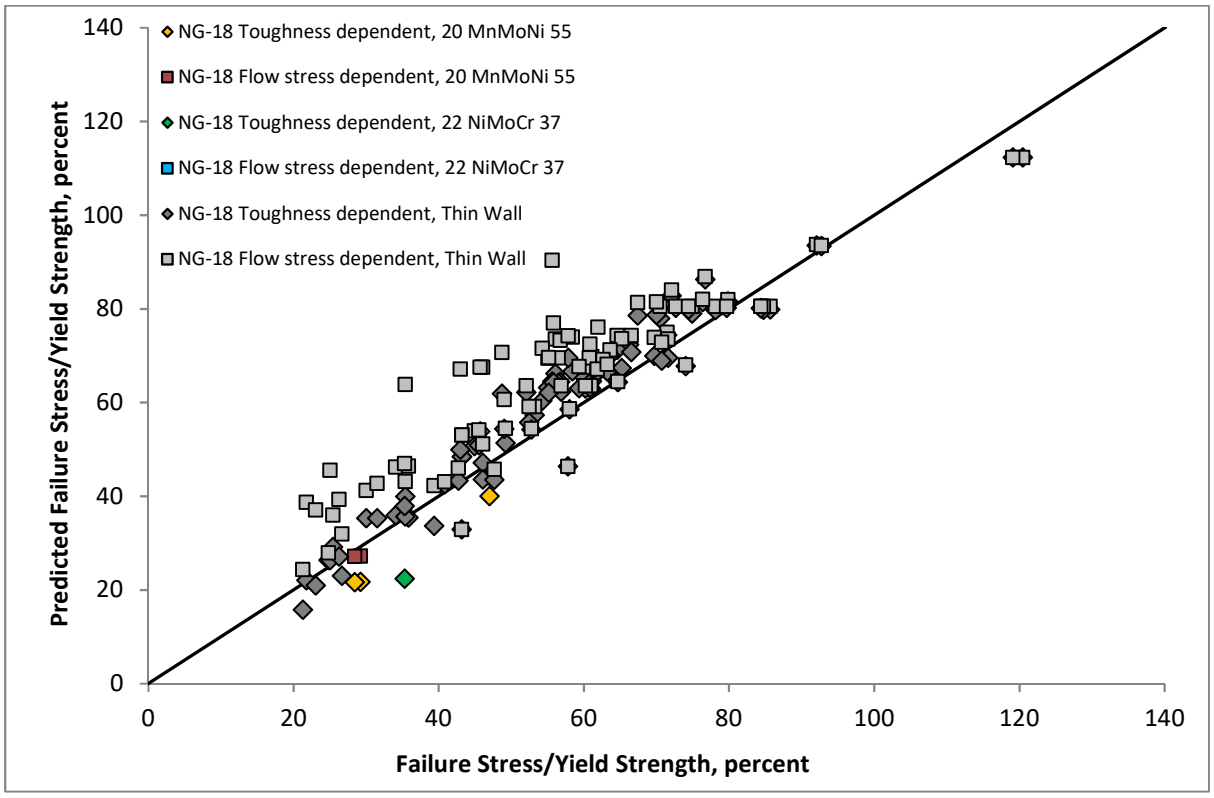

Figure 6 Predicted versus Actual Failure Stress for Axial Through-Wall Defects in Thick and Thin Wall Pipe Sections According to the Toughness and Flow Stress Dependent Forms of the NG-18 Equations, Sturm and Stoppler, Kiefner et al.

In summary, Figure 5 and Figure 6 suggest that the flow stress dependent NG-18 equation is a valid assessment method for through-wall defects in pipelines up to at least 47.2 mm wall thickness with a full-size equivalent upper shelf Charpy V-notch impact energy of at least 50 J.

4.2. PART-WALL DEFECTS

4.2.1. PART-WALL FAILURE DATA

The experimental failure data (Staat, 2004) available for burst tests with part-wall defects on thick wall vessels originates from Eiber et al. in 1971 (Eiber et al., 1971), Wellinger and Sturm in 1971 (Wellinger and Sturm, 1971), Sturm and Stoppler in 1990 (Sturm and Stoppler, 1990), Keller at al. in 1987 (Keller, Junker and Merker, 1987) and Mannucci et al. in 2001 (Mannucci, Demofonti, Harris, Barsanti and Hillenbrand, 2001).

As reported by Eiber et al. (Eiber et al., 1971), four tests were performed on vessels constructed from A 106 B grade steel, two tests were performed on vessels constructed from Type 316 stainless steel and one test was performed on a vessel constructed from A 316 stainless steel. Details of the vessels and tests are summarised in Table 8.

Input	Value
External Diameter (mm)	609.6
Wall Thickness Range (mm)	38.1 – 43.7
Material Grade	A 106 B, Type 316, A 316
Yield Strength (Nmm^{-2})	155, 241
Tensile Strength (Nmm^{-2})	426, 570
Charpy V-Notch Impact Energy (J) Full-Size Range	81 – 200
Defect Length Range (2c) (mm)	76 – 361
Defect Depth Range (d) (% wall thickness)	47 – 88

Table 8: Thick Wall, Part-Wall Burst Test Vessel Details, Eiber et al. 1971

Wellinger and Sturm (1971) report 23 tests that were performed on vessels constructed from St 35 grade steel and two tests that were performed on vessels constructed from FB 70 grade steel. Details of the vessels and tests are summarised in Table 9.

Input	Value
External Diameter (mm)	88.9
Wall Thickness (mm)	22.2
Material Grade	St 35, FB 70
Yield Strength Range (Nmm^{-2})	199 – 473
Tensile Strength Range (Nmm^{-2})	438 – 614
Charpy V-Notch Impact Energy (J) Full-Size Range	56 – 71
Defect Length Range (2c) (mm)	40.5 – 123
Defect Depth Range (d) (% wall thickness)	18.9 – 88.7

Table 9: Thick Wall, Part-Wall Burst Test Vessel Details, Wellinger and Sturm 1971

As stated by Sturm and Stoppler (1990), four tests were performed on vessels constructed from 20 MnMoNi 55 grade steel and three tests were performed on vessels constructed from 22 NiMoCr 37 grade steel. Details of the vessels and tests are summarised in Table 10.

Input	Value
External Diameter (mm)	797.9, 793.9
Wall Thickness (mm)	47.2
Material Grade	20 MnMoNi 55, 22 NiMoCr 37
Yield Strength (Nmm^{-2})	428, 417
Tensile Strength (Nmm^{-2})	622, 605
Charpy V-Notch Impact Energy (J) Full-Size	150, 50
Defect Length Range (2c) (mm)	709 – 1500
Defect Depth Range (d) (% wall thickness)	74 – 81

Table 10: Thick Wall, Part-Wall Burst Test Vessel Details, Sturm and Stoppler 1990

According to Keller, Junker and Merker (1987), two tests were performed on vessels constructed from 34 CrMo 4 grade steel. Details of the vessels and tests are summarised in Table 11.

Input	Value
External Diameter (mm)	564.8, 565.4
Wall Thickness (mm)	20.4, 21.7
Material Grade	34 CrMo 4
Yield Strength (Nmm^{-2})	878, 866
Tensile Strength (Nmm^{-2})	990, 979
Charpy V-Notch Impact Energy (J) Full-Size	64, 65
Defect Length (2c) (mm)	48, 32.5
Defect Depth (d) (% wall thickness)	78.9, 66.8

Table 11: Thick Wall, Part-Wall Burst Test Vessel Details, Keller et al. 1987

As reported by Mannucci (Mannucci, et al., 2001), two tests were performed on vessels constructed from API 5L X100 grade steel. Details of the vessels and tests are summarised in Table 12.

Input	Value
External Diameter (mm)	1422.4
Wall Thickness (mm)	19.25, 20.1
Material Grade	API 5L X100
Yield Strength (Nmm^{-2})	740, 795
Tensile Strength (Nmm^{-2})	774, 840
Charpy V-Notch Impact Energy (J) 2/3-Size	261, 171
Defect Length (2c) (mm)	180, 385
Defect Depth (d) (% wall thickness)	54, 18.9

Table 12: Thick Wall, Part-Wall Burst Test Vessel Details, Mannucci et al. 2001

Data from burst tests of part-wall defects on thin wall vessels has also been included in order to provide a comparison. This data originates from Battelle in 1973 (Kiefner, Maxey, Eiber and Duffy, 1973) and includes data from 33 burst tests of part-wall defects on thin wall pressure vessels. These tests were performed for a range of different vessels and parameters. Details are summarised in Table 13.

Input	Value
External Diameter Range (mm)	762 – 1067
Wall Thickness Range (mm)	9.1 – 15.6
Yield Strength Range (Nmm^{-2})	379 – 510
Tensile Strength Range (Nmm^{-2})	531 – 634
Charpy V-Notch Impact Energy (J) Full-Size	24 – 69
Defect Length Range (2c) (mm)	64 – 610
Defect Depth Range (d) (% wall thickness)	25 – 92

Table 13: Thin Wall, Part-Wall Burst Test Vessel Details, Kiefner et al., 1973

4.2.2. FAILURE DATA COMPARISON

A comparison has been made between the actual failure stresses for the set of axial part-wall defects in thick wall pressure vessels and those predicted for the same set of defects by the part-wall toughness dependent and flow stress dependent NG-18 equations. The results are shown in Figures 7 to 10. The failure stress is assumed to be the hoop stress at the failure pressure.

For the experimental data considered in Figure 7, both the toughness and flow stress dependent forms of the NG-18 equations produce reasonably accurate results. Furthermore, the predictions of each form of the NG-18 equation are very similar. Figure 8 in particular, shows the predictions of the toughness and flow stress dependent forms of the NG-18 equation to be almost identical for this particular set of experimental data.

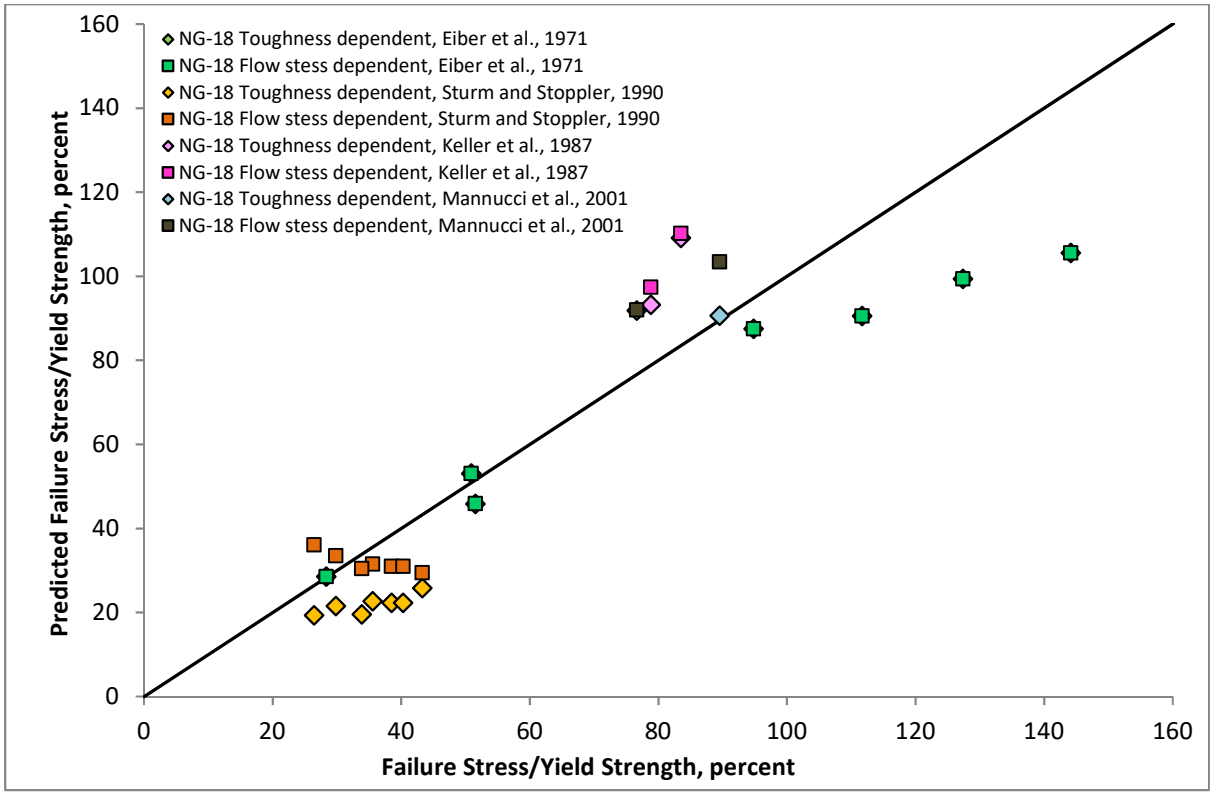

476

477 Figure 7 Predicted versus Actual Failure Stress for Axial Part-Wall Defects in Thick Wall Pipe
478 Sections According to the Toughness and Flow Stress Dependent Forms of the NG-18
479 Equations, Eiber et al., Sturm and Stoppler, Keller and Mannucci et al.

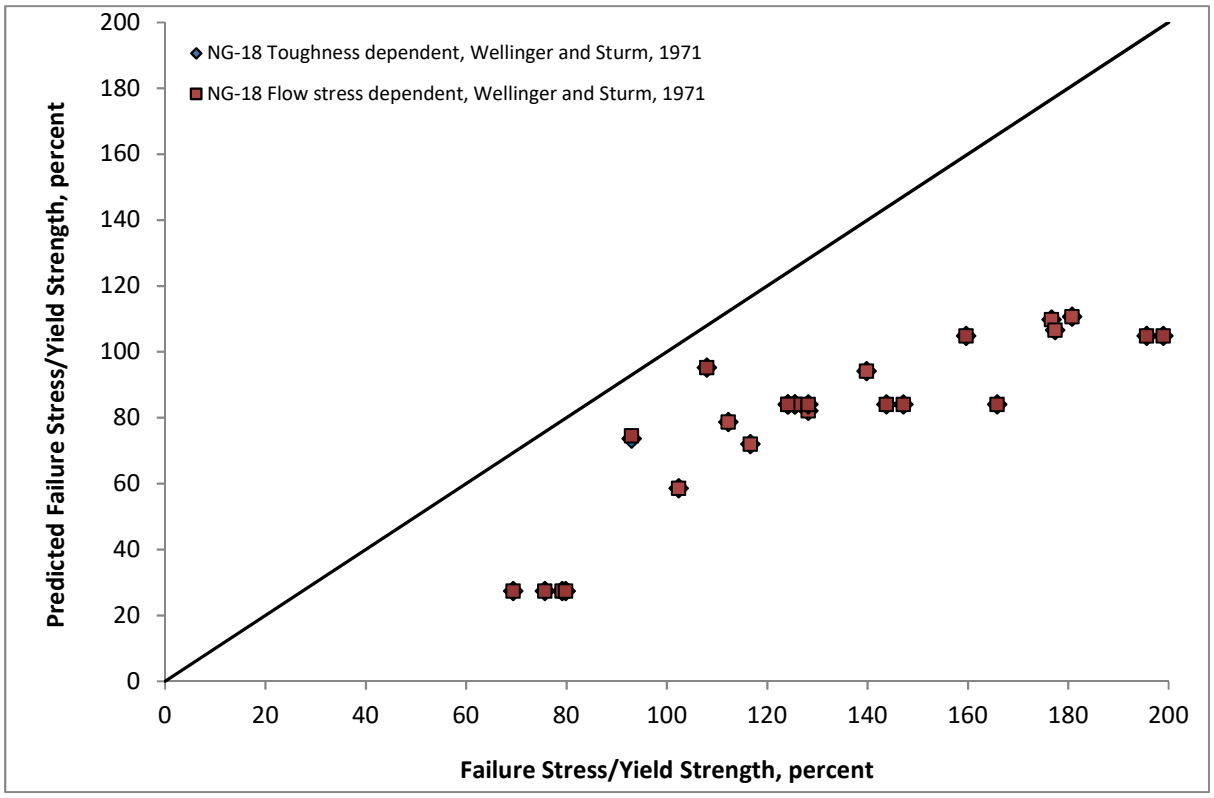

480

Figure 8 Predicted versus Actual Failure Stress for Axial Part-Wall Defects in Thick Wall Pipe Sections According to the Toughness and Flow Stress Dependent Forms of the NG-18 Equations, Wellinger and Sturm

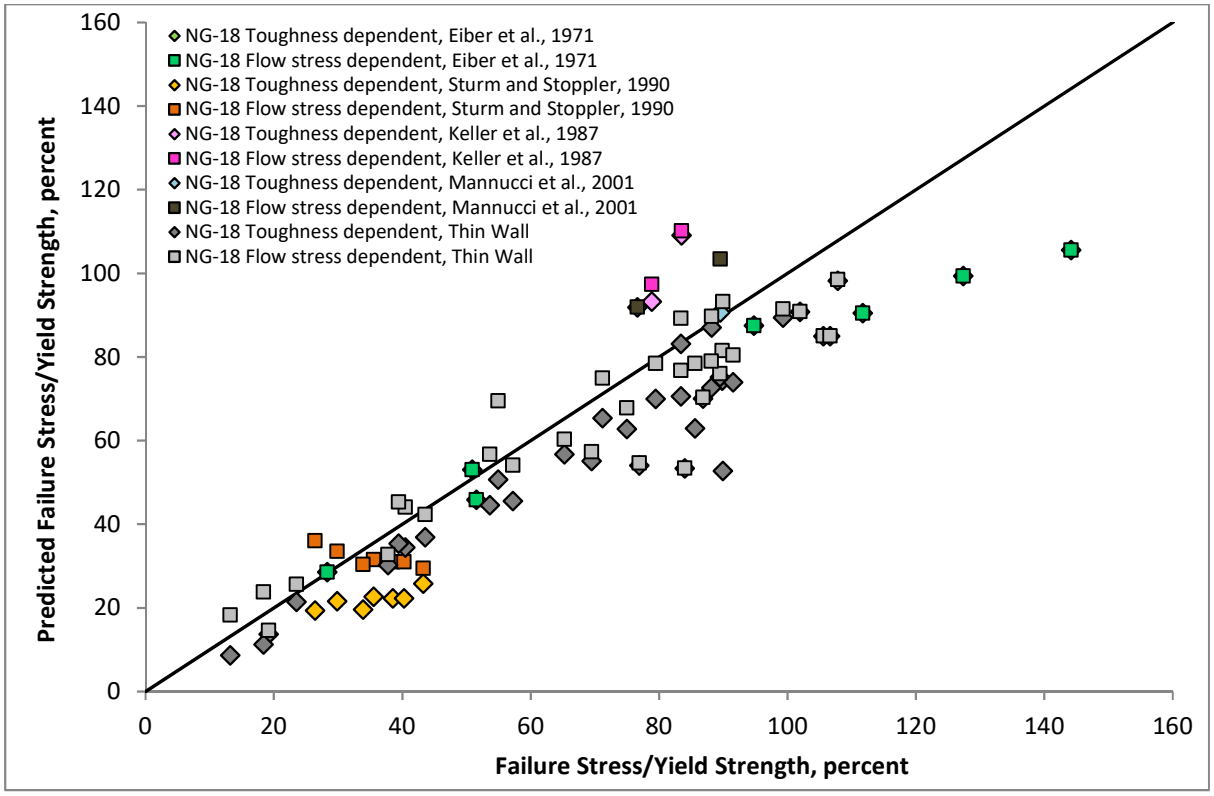

Figure 9 Predicted versus Actual Failure Stress for Axial Part-Wall Defects in Thick and Thin Wall Pipe Sections According to the Toughness and Flow Stress Dependent Forms of the NG-18 Equations, Eiber et al., Sturm and Stoppler, Keller and Mannucci et al., Kiefner et al.

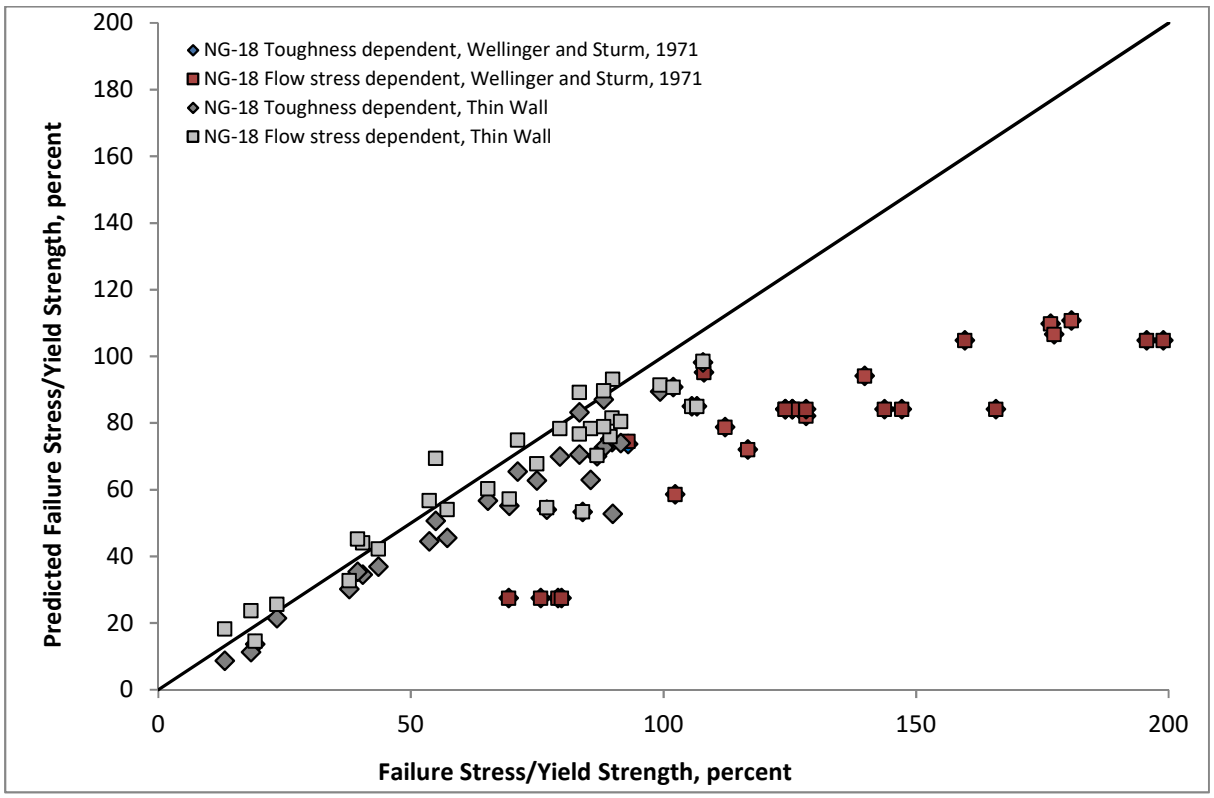

Figure 10 Predicted versus Actual Failure Stress for Axial Part-Wall Defects in Thick and Thin Wall Pipe Sections According to the Toughness and Flow Stress Dependent Forms of the NG-18 Equations, Wellinger and Sturm, Kiefner et al

Figure 9 and Figure 10 include thin wall failure data from Battelle in 1973 (Table 13). In Figure 9, the thick wall data for NG-18 is contained within the scatter of the data points of the thin wall data. In Figure 10, the thick wall data for the NG-18 equation does not lie within the scatter of the data points of the thin wall data and they tend to be much lower than the actual failure values. The reason for this is the small pipe diameter to wall thickness ratio of the vessels used in these tests, that emphasises the conservative nature of Barlow's equation for thin wall pipelines when applied to thick wall pipelines.

In summary, Figures 7 to 10 suggest that the flow stress dependent NG-18 equation is a valid assessment method for part-wall defects in pipelines up to at least 47.2 mm wall thickness with a full-size equivalent upper shelf Charpy V-notch impact energy of at least 50 J.

5. CONCLUSIONS AND RECOMMENDATIONS

The component parts of the through-wall and part-wall NG-18 equations and BS 7910 were compared and it was found that the factor M_T for though-wall defects and M_P for part-wall defects in the NG-18 equations are very close to the reference stress solutions in BS 7910, which are applicable to thick wall pipe. Furthermore, calculations for example defects showed that the effect of the other differences between the two assessment methods, such as the inclusion of the bending stress in BS 7910, are small and remain so even when the pipeline wall thickness is increased. Comparisons with experimental failure data for thick wall vessels also showed that the flow stress dependent NG-18 equations are valid assessment methods for through-wall and part-wall defects in pipelines up to a wall thickness of at least 47.2 mm, when the full-size equivalent upper shelf Charpy V-notch impact energy is at least 50 J.

These findings suggest that, in principle, the flow stress dependent NG-18 equations may be used as limit state functions in the established failure frequency method used to calculate the failure frequency due to third party external interference for high toughness, thick wall pipelines such as those required for dense phase CO_2 pipelines.

For modern, high toughness line pipe steel, defect failure will occur as a result of plastic collapse rather than fracture. In a plastic collapse failure, the fracture toughness, by definition, has no effect. The flow stress dependent NG-18 equations should be suitable for application to thick wall CO_2 pipelines, provided the pipe material has a high toughness. However, it is unclear as to where the boundary between high (entirely plastic collapse) and low toughness (fracture/plastic collapse combination) lies. Therefore, further study is required to determine the minimum toughness for failure to be controlled by plastic collapse.

It is recommended that further work is carried out in order to determine the toughness limit at which it is acceptable to use the flow stress dependent form of the NG-18 equations.

6. ACKNOWLEDGEMENTS

This work has been conducted under the auspices of the National Grid COOLTRANS research programme and the authors gratefully acknowledge the financial support of National Grid for this research.

The Don Valley CCS Project was co-financed by the European Union's European Energy Programme for Recovery. The sole responsibility for this publication lies with the authors. The European Union is not responsible for any use that may be made of the information contained therein.

7. REFERENCES

BSI, 1991. Guidance on Methods for Assessing the Acceptability of Flaws in Fusion Welded Structures, PD 6493:1991, British Standards Institution, London UK, 1991.

BSI, 2013. BS 7910:2013+A1:2015 Guide to methods for assessing the acceptability of flaws in metallic structures. December 2013. British Standards Institution.

BSI, 2015. PD 8010: Part-1:2015+A1:2016 Pipeline systems. Steel pipelines on land. Code of practice. March 2015. British Standards Institution.

Cooper, R. and Barnett, J., 2014. The COOLTRANS Research Programme: Learning for the Design of CO_2 Pipelines. 10th International Pipeline Conference. Paper No. IPC2014-33370.

Corder, I., Fearnehough, G.D., and Knott, R.N., 1992, Pipeline Design Using Risk Based Criteria, Institute of Gas Engineers 129th Annual General Meeting and Spring Conference, Communication 1492, Eastbourne, UK.

Corder, I., 1995, The Application of Risk Techniques to the Design and Operation of Pipelines, C502/016/95, Proceedings of International Conference on Pressure Systems: Operation and Risk Management, Institution of Mechanical Engineers, London, October 1995, pp. 113– 125.

Cosham, A., Haswell, J. and Jackson, N., 2008, Reduction Factors for Estimating the Probability of Failure of Mechanical Damage due to External Interference, IPC2008-64345, Proceedings of IPC2008, 7th International Pipeline Conference, American Society of Mechanical Engineers, September 29th to October 3rd, Calgary, Alberta, Canada, 2008.

Cosham, A., Hopkins, P., Leis, B., 2012. Crack-Like Defects in Pipelines: The Relevance of Pipeline-Specific Methods and Standards, IPC2012-90459, Proceedings of the 2012 9th International Pipeline Conference September 24-28th, 2012, Calgary, Alberta, Canada.

Department for Business, Energy & Industrial Strategy, 2017. The Clean Growth Strategy Leading the way to a low carbon future, HM Government, Crown copyright.

Downie, M.J., Race, J.M., Seevam, P.N., 2007. SPE 109060: Transport of CO_2 for Carbon Capture and Storage in the UK, Offshore Europe 2007. Aberdeen, Scotland, UK, 4-7th September 2007. SPE International.

Eiber, R.J., Maxey, W.A., Duffy, A.R., and Atterbury, T.J., 1971. Investigation of initiation and extent of ductile pipe rupture Final report, Task 17 (BMI--1908). United States.

Folias, E.S. 1975. On the Fracture of Nuclear Reactor Tubes, Paper C4/5, Transactions of Third International Conference on Structural Mechanics in Reactor Technology (SMiRT).

Goodfellow, G., Turner, S., Haswell, J., Espiner, R., 2012. IPC2012-90247: An Update to the UKOPA Pipeline Damage Distributions, 9th International Pipeline Conference. Calgary, Alberta, Canada, September 24-28th 2012.

Hahn, G.T., Sarrate, M., Rosenfield, A.R., 1969. Criteria for Crack Extension in Cylindrical Pressure Vessels, International Journal of Fracture Mechanics, Vol. 5 No. 3, 1969, pp. 187-210.

HSE, 2001. An assessment of measures in use for gas pipelines to mitigate against damage caused by third party activity. Contract Research Report 372/2001, Prepared by WS Atkins Consultants Ltd for the Health and Safety Executive, HMSO, London 2001.

IGEM, 2016, IGEM/TD/1 Edition 5 with amendments July 2016: Steel Pipelines and Associated Installations for High Pressure Gas Transmission. Institution of Gas Engineers and Managers.

IGEM, 2013, Assessing the risks from high pressure Natural Gas pipelines, IGEM/TD/2 Edition 2, Institution of Gas Engineers and Managers.

Keller, H.P., Junker, G., and Merker, W., 1987. Fracture Analysis of Surface Cracks in Cylindrical Pressure Vessels Applying the Two Parameter Fracture Criterion (TPFC), International Journal of Pressure Vessels and Piping, Vol. 29, 1987, pp 113-153.

Kiefner, J.F., 1969. Fracture Initiation, Paper G, Proceedings of the 4th Symposium on Line Pipe Research, Pipeline Research Committee of the American Gas Association, Dallas, Texas, USA, AGA Catalogue No. L30075, 18-19th November, 1969, pp. G1-G36.

Kiefner, J.F., Maxey, W.A., Eiber, R.J., and Duffy, A.R., 1973. The Failure Stress Levels of Flaws in Pressurised Cylinders, ASTM STP 536, American Society for Testing and Materials, Philadelphia, 1973, pp. 461-481.

Lamé, G. and Clapeyron, B.P.E., 1833. Mémoire sur l'équilibre intérieur des corps solides homogènes [Memoir on the internal balance of homogeneous solid bodies]. In Mémoires de l'Académie (royale) des sciences de l'Institut (imperial) de France, Mémoires présentés par divers savans à l'Académie royale des sciences de l'Institut de France, et imprimés par son ordre. Sciences mathématiques et physiques [Memoirs presented by various scholars to the Royal Academy of Sciences of the Institut de France, and printed by his order: Mathematical and physical sciences], 4: 463-562.

Lyons, C., Haswell, J. V., Hopkins, P., Ellis, R., Jackson, N., 2008. A Methodology for the Prediction of Pipeline Failure Frequency Due to External Interference, Proceedings of the Pipeline Pigging and Integrity Management Conference 2009. IPC2008-64375.

Lyons, C. J., Race, J. M., Wetenhall, B., Chang, E., Hopkins, H. F. and Barnett, J., 2019. Assessment of Failure Frequency Methodology for Dense Phase Carbon Dioxide Pipelines, International Journal of Greenhouse Gas Control 87 (2019) 112–120.

Mannucci, G., Demofonti, G., Harris, D., Barsanti, L., Hillenbrand, H.-G., 2001. Fracture Properties of API X100 Gas Pipeline Steels. EP-TP39–01en, Europipe, Ratingen, Germany.

Maxey, W.A., Kiefner, J.F., Eiber, R.J., and Duffy, A.R., 1972. Ductile Fracture Initiation, Propagation and Arrest in Cylindrical Vessels, ASTM STP 514, American Society for Testing and Materials, Philadelphia, 1972, pp. 70-81.

Noothout, P., Wiersma, F., Hurtado, O., Macdonald, D., Kemper, J., van Alphen, K., 2014. CO_2 Pipeline infrastructure – lessons learnt Energy Procedia 63 (2014) 2481 – 2492.

Staat, M., 2004. Plastic Collapse Analysis of Longitudinally Flawed Pipes and Vessels, Nuclear Engineering and Design 234 (2004) 25-43.

Sturm, D. and Stoppler, W., 1990. Strength Behaviour of Flawed Pipes under Internal Pressure and External Bending Moment: Comparison between Experiment and Calculation, International Journal of Pressure Vessels and Piping, Vol. 43, 1990, pp 351-366.

UKOPA, 2019. UKOPA Pipeline Fault Database – Pipeline Product Loss Incidents (1962 – 2017), UKOPA/RP/18/002, March 2019.

Wellinger, K. and Sturm, D., 1971. Festigkeitsverhalten von zylindrischen Hohlkörpern. Fortschr. Ber. VDI-Z. Reihe 5, Nr. 13, VDI-Verlag, Düsseldorf.